Journal of Chromatography A, 1218 (2011) 4009–4024

Contents lists available at ScienceDirect

Journal of Chromatography A

journal homepage: www.elsevier.com/locate/chroma

Statistical theory of linear adsorption capillary chromatography with porous-layer stationary phase

Yinliang Chen*

Institute of Nuclear Physics and Chemistry, Chinese Academy of Engineering Physics, Mianyang, Sichuan 621900, China

ARTICLE INFO

Article history:
Received 28 January 2011
Received in revised form 22 April 2011
Accepted 26 April 2011
Available online 6 May 2011

Keywords:
Chromatography
Capillary
Adsorption
Moment
Retention time
Elution curve
Porous layer
Mathematica

ABSTRACT

A set of accurate expressions of elution-curve moments are derived from the moments of residence time and displacement in a step based on probability theory. Then the problems about residence time and displacement in a step of a solute molecule in the porous layer of capillary columns and in the moving mobile phase are described by a set of mass-balance equations respectively. The set of equations are solved in Fourier–Laplace domain, and the characteristic functions of residence time of a step, as well as the moments, are obtained by means of computing software Mathematica. At last, using numerical inverse Laplace transform, the elution curves for various conditions are calculated. In the case of large desorption constant the results entirely coincide with those of mass-balance-equation theory and in the case of small desorption constant they are equivalent to those of stochastic theory.

1. Introduction

Because of the extreme complexity of chromatographic processes, it is difficult to obtain an accurate elution curve by pure theoretical calculation. Giddings and Eyring [1,2] gave an analytical expression of elution curves for pure-rate-controlling adsorption chromatography. However, in most cases, diffusions cannot be ignored. Cavazzini, Felinger and Dondi et al. [3–6] used characteristic function theory (CF theory) to obtain an expression containing axial diffusions in mobile phases in frequency domain, then to give the elution curves in time domain by numerical inversion. In the model of Cavazzini et al., the diffusions in stationary phases and the lateral diffusions in mobile phases are not considered. This is correct for slow-desorption processes, because in these processes diffusions do not play a major role. In most cases, elution curves can be approached by Cram–Charlier series [7] or Edgeworth–Cramer series [8,9], or simply by Gaussian distribution. In this way calculating an elution curve is reduced to calculating its retention time and moments. However, there have not been general moment expressions suitable for various desorption constants. Moreover while the skew of elution curves exceeds 1 much, they are hard to be expanded in Cram–Charlier series or similar series at all.

We have presented a new stochastic theory based on mass balance principle, in which the lateral diffusions are involved [10], and used in linear capillary chromatography with uniform stationary phases and with multiple-site nonporous layer stationary phases [11,12]. But the case of porous layers is much more complex. In this paper we intend to think over all the factors which affect the linear capillary adsorption chromatography with porous layers, including the desorption rates and both the axial and the lateral diffusions in stationary phases and mobile phases, as well as the structure of stationary phases, the pressure drop in mobile phases and so on. Starting from a series of basic parameters such as the column parameters (the column length, the column radius, the thickness of porous layer, the porosity and the specific surface area), the operating conditions (the linear flow rate, the time distribution of sample injection, the gas pressure drop along the column) and the physicochemical parameters of solutes (the desorption rate constants, the distribution constants, the diffusion coefficients), we calculate the elution curves and their moments, and compare them with those in literature. However, in this paper we will still limit the study only in the capillary columns, not concern the more complex packed columns.

2. General Laplace transform of elution curves

According to the random walk model [13], a solute molecule in a column can be imagined to move in the way of

* Corresponding author. Tel.: +86 816 2486230.
E-mail address: chen_yinliang@live.cn

0021-9673/$ – see front matter © 2011 Elsevier B.V. All rights reserved.
doi:10.1016/j.chroma.2011.04.072

moving–adsorbing–moving alternately progressing and to go from the inlet to the outlet step by step. The processes can be expressed by following formula [10–12]:

$$\begin{cases} \tau_c = \sum_{j=1}^{n} \tau_j \\ \sum_{j=1}^{n} \eta_j \le L < \sum_{j=1}^{n+1} \eta_j \end{cases} \tag{1}$$

where n is the number of steps for a molecule to pass through a column, τ_c represents the total time for a molecule to spend in the column, τ_j and η_j are the residence time and displacement in the jth step respectively. Obviously, n, τ_c, τ_j and η_j are all random. The second formula in Eq. (1) represents the condition that a molecule leaves the column. Denote $\sum_{j=1}^{n}\tau_j$ and $\sum_{j=1}^{n}\eta_j$ of given n by τ'_n and η'_n respectively, and denote the probability density function (PDF) of (η'_n, τ'_n) by $f_{\eta'_n\tau'_n}(z, t)$ and the PDF of η_{n+1} by $f_\eta(z)$. Because of independence of η_{n+1} and (η'_n, τ'_n) in linear chromatography, there is

$$\begin{aligned} &P_n(\tau'_n \le t, \eta'_n \le L < \eta'_n + \eta_{n+1}) \\ &= \int_0^t \left(\int_{z'\le L<z'+z''} f_{\eta'_n\tau'_n}(z', t') f_\eta(z'') dz' dz'' \right) dt' \\ &= \int_0^t \int_{-\infty}^{L} f_{\eta'_n\tau'_n}(z', t') dz' dt' \int_{L-z'}^{\infty} f_\eta(z'') dz'' \end{aligned} \tag{2}$$

where $P_n(\tau'_n \le t, \eta'_n \le L < \eta'_n + \eta_{n+1})$ represents the probability of $\tau'_n \le t$, $\eta'_n \le L$ and $\eta'_n + \eta_{n+1} > L$. Let $f_{\eta\tau}(z, t)$ be the PDF of the displacement and residence time in an arbitrary step and $\tilde{f}_{\eta\tau}(\omega, p)$ be its Fourier–Laplace transform. Generally, we add a random variable to the subscript of a function to indicate that the function is a PDF of the variable and add a wave above the function symbol to represent its Laplace or Fourier–Laplace transform.

$$\tilde{f}_{\eta\tau}(\omega, p) = \int_0^\infty \int_{-\infty}^{\infty} f_{\eta\tau}(z, t) e^{i\omega z - pt} dz dt \tag{3}$$

where i is the imaginary unit. Then we have

$$\tilde{f}_{\eta'_n\tau'_n}(\omega, p) = (\tilde{f}_{\eta\tau}(\omega, p))^n \tag{4}$$

The PDF of τ'_n is given by

$$\begin{aligned} f_{\tau'_n}(t) &= \frac{d}{dt} P_n(\tau'_n \le t, \eta'_n \le L < \eta'_n + \eta_{n+1}) \\ &= \int_{-\infty}^{L} f_{\eta'_n\tau'_n}(z', t) dz' \int_{L-z'}^{\infty} f_\eta(z'') dz'' \end{aligned} \tag{5}$$

Making Fourier–Laplace transform of $f_{\tau'_n}(t)$ with respect to L and t, we have

$$\widetilde{f}_{\tau'_n}(\omega, p) = \int_0^\infty \int_{-\infty}^{\infty} f_{\tau'_n}(t) e^{i\omega L - pt} dL dt = g(\omega) \widetilde{f}_\eta(\omega, p))^n \tag{6}$$

where

$$g(\omega) = \frac{1}{i\omega} \int_0^\infty f_\eta(z'') (e^{i\omega z''} - 1) dz'' \tag{7}$$

The practical residence time should include all possible steps, so its PDF should be

$$f_{\tau_c}(t) = \sum_{n=0}^{\infty} f_{\tau'_n}(t) \tag{8}$$

The function of $f_{\tau_c}(t)$ contains the variable of L. Its Fourier–Laplace transform with respect to L and t is

$$\widetilde{f}_{\tau_c}(\omega, p) = \int_0^\infty \int_{-\infty}^{\infty} f_{\tau_c}(t) e^{i\omega z - pt} dz dt = \sum_{n=0}^{\infty} \widetilde{f}_{\tau'_n}(\omega, p) = \frac{g(\omega)}{1 - \widetilde{f}_{\eta\tau}(\omega, p)} \tag{9}$$

The Laplace transform of $f_{\tau_c}(t)$ with respect to t can be given by inverse transform of $\widetilde{f}_{\tau_c}(\omega, p)$ with respect to ω:

$$\tilde{f}_{\tau_c}(p) = \frac{1}{2\pi} \int_{-\infty}^{\infty} \frac{g(\omega)}{1 - \widetilde{f}_{\eta\tau}(\omega, p)} e^{-i\omega L} d\omega \tag{10}$$

The integrand of Eq. (10) has a first pole at

$$\omega = \omega(p) \tag{11}$$

which is determined by

$$\widetilde{f}_{\eta\tau}(\omega, p) = 1 \tag{12}$$

Using the residue theorem, the integral of Eq. (10) is calculated approximately to be

$$\tilde{f}_{\tau_c}(p) = e^{-i\omega(p)L} \tag{13}$$

Here we omit a factor related to the residue of $g(\omega)/(1 - \tilde{f}_{\eta\tau}(\omega, p))$ at $\omega = \omega(p)$, for not too short columns the factor has no influence on results. So far, we obtain the Laplace transform of elution curves without any additional conditions.

3. Residence time and displacement in a step

A step defined in this paper contains two parts: corresponding to the static zone and to the moving zone respectively. Let (η_s, τ_s) be the displacement and the residence time in the static zone per step, (η_m, τ_m) be the corresponding ones in the mobile zone, we have

$$\begin{cases} \tau = \tau_s + \tau_m \\ \eta = \eta_s + \eta_m \end{cases} \tag{14}$$

Movement of solute molecules in static zones includes two parts: diffusion in porous layers and adsorption–desorption on solid surfaces. The corresponding displacements and residence times are denoted by (η_{s1}, τ_{s1}) and (η_{s2}, τ_{s2}) respectively. Obviously all the (η_{s1}, τ_{s1}), (η_{s2}, τ_{s2}) and (η_m, τ_m) are random and characterized by their PDFs. In our model the general diffusion-drift equations are used to determine the PDFs [11,12]. In the case of porous layers, the diffusion in pores can be approached by the diffusion in homogeneous media, see appendix A. Thus taking into account the adsorption–desorption on solid surfaces, the mass balance equations of solute molecules in static zones can be simplified as

$$\begin{cases} \dfrac{\partial C}{\partial t} = D_{sr}\left(\dfrac{\partial^2 C}{\partial r^2} + \dfrac{1}{r}\dfrac{\partial C}{\partial r}\right) + D_{sa}\dfrac{\partial^2 C}{\partial z^2} + \varepsilon_s \sum_j (k_{dj} C_{sj} - k'_{aj} C) \\ \dfrac{\partial C_{sj}}{\partial t} = -k_{dj} C_{sj} + k'_{aj} C \\ C(r, z, t)\big|_{t=0} = C_{sj}(r, z, t)\big|_{t=0} = 0 \\ \left.\dfrac{\partial C}{\partial r}\right|_{r=R+d_l} = 0 \\ -D_{sr}\left.\dfrac{\partial C(r, z, t)}{\partial r}\right|_{r=R} = \dfrac{\delta(t)\delta(z)}{2\pi R} - \dfrac{\nu}{2} C(R, z, t) \end{cases} \tag{15}$$

where $C(r, z, t)$ represents the concentration of solute molecules in pores, $C_{sj}(r, z, t)$ the amount adsorbed by the site of type j per area of solid surfaces, C and C_{sj} are their abbreviation respectively,

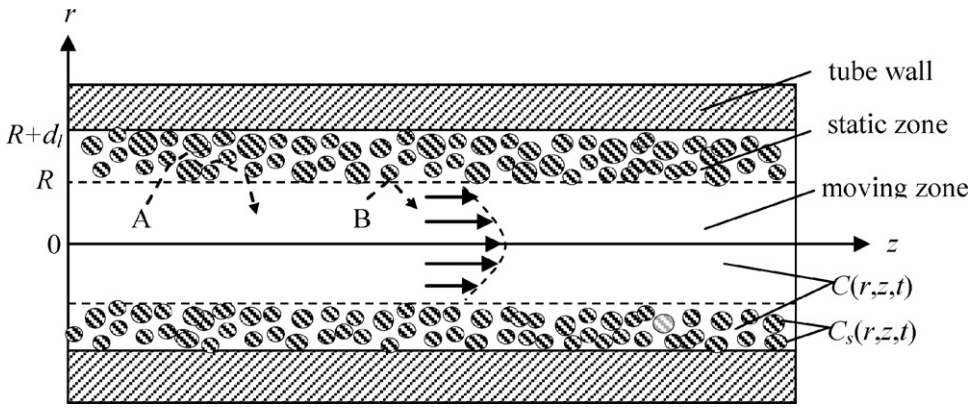

Fig. 1. Schematic of capillary columns with porous layers. (A) a solute molecule entering the pores. (B) a solute molecule hitting the outside surface.

D_{sa} the axial equivalent diffusion coefficient in porous media, D_{sr} the corresponding radial equivalent diffusion coefficient, z the axial coordinate of the capillary column, r the radial coordinate, t time, R the inner radius of the column, d_l the thickness of the porous layer, ε_s the surface area occupied by per unit volume of pores, k_{dj} the desorption rate constant of site j, k'_{aj} the adsorption reaction rate constant, $\delta(z)$ and $\delta(t)$ are Dirac-δ function, v the mean velocity of molecules. The last equation in Eq. (15) means that at $t=0$ and $z=0$ there is a unit amount of solute molecules entering the porous layer, and at $t>0$ at z there is an outgoing molecular flow with intensity of $vC(R, z, t)/2$. Since the in-coming molecules are supposed to be one unit amount and to concentrate at $t=0$ and $z=0$, $2\pi R\, vC(R, z, t)/2$ is equal to the PDF of the residence time τ_{s1} and displacement η_{s1} of a molecule after entering pores, i.e.

$$f_{\eta_{s1}\tau_{s1}}(z,t) = \pi R v C(R,z,t) \tag{16}$$

Making Fourier–Laplace transform, we have

$$\begin{cases} p\tilde{C} = D_{sr}\left(\dfrac{\partial^2\tilde{C}}{\partial r^2} + \dfrac{1}{r}\dfrac{\partial\tilde{C}}{\partial r}\right) - D_{sa}\omega^2\tilde{C}) + \varepsilon_s\displaystyle\sum_j (k_{dj}\tilde{C}_{sj} - k'_{aj}\tilde{C}) \\ p\tilde{C}_{sj} = -k_{dj}\tilde{C}_{sj} + k'_{aj}\tilde{C} \quad j = 1, 2, \cdots \\ \left.\dfrac{\partial\tilde{C}}{\partial r}\right|_{r=R+d_l} = 0 \\ \left.-D_{sr}\dfrac{\partial\tilde{C}}{\partial r}\right|_{r=R} = \dfrac{1}{2\pi R} - \dfrac{v}{2}\tilde{C}(R,\omega,p) \end{cases} \tag{17}$$

where

$$\tilde{C}_{sj} = \int_0^\infty\int_{-\infty}^\infty C_{sj}(r,z,t)e^{i\omega z - pt}dzdt \tag{18}$$

$$\tilde{C} = \tilde{C}(r,\omega,p) = \int_0^\infty\int_{-\infty}^\infty C(r,z,t)e^{i\omega z - pt}dzdt \tag{19}$$

Eliminating $\tilde{C}_{sj}$ from Eq. (17), it gives

$$\begin{cases} D_{sr}\left(\dfrac{\partial^2\tilde{C}}{\partial r^2} + \dfrac{1}{r}\dfrac{\partial\tilde{C}}{\partial r}\right) + A\tilde{C} = 0 \\ \left.\dfrac{\partial\tilde{C}}{\partial r}\right|_{r=R+d_l} = 0 \\ \left.-D_{sr}\dfrac{\partial\tilde{C}}{\partial r}\right|_{r=R} = \dfrac{1}{2\pi R} - \dfrac{v}{2}\tilde{C}(R,\omega,p) \end{cases} \tag{20}$$

where

$$A = -D_{sa}\omega^2 - p\left(\varepsilon_s\sum_j\frac{k'_{aj}}{p+k_{dj}} + 1\right) \tag{21}$$

From this the transform of $f_{\eta_{s1}\tau_{s1}}(z,t)$ is given as follows

$$\tilde{f}_{\eta_{s1}\tau_{s1}}(\omega,p) = \int_0^\infty\int_{-\infty}^\infty f_{\eta_{s1}\tau_{s1}}(z,t)e^{i\omega z - pt}dzdt = \pi R v\tilde{C}(R,\omega,p) \tag{22}$$

When a group of solute molecules crosses the interface of the two zones from the moving one, only a portion equal to the porosity ε can come into the pores. And the rest of $1-\varepsilon$ directly hit the out surface, see Fig. 1. The PDF of the residence time of direct hitting has been given by Ref. [11]. However the residence time from direct hitting is much less than that from coming into pores and reasonably ignored. In this way the PDF of the displacement and residence time in the static zone in an arbitrary step can be written as

$$f_{\eta_s\tau_s}(z,t) = \varepsilon f_{\eta_{s1}\tau_{s1}}(z,t) + (1-\varepsilon)\delta(t)\delta(z) \tag{23}$$

$$\tilde{f}_{\eta_s\tau_s}(\omega,p) = \varepsilon\tilde{f}_{\eta_{s1}\tau_{s1}}(\omega,p) + (1-\varepsilon) \tag{24}$$

Movement of solute molecules in the moving zone includes the diffusion and drift. From this the corresponding mass balance equations are obtained as follows

$$\begin{cases} \dfrac{\partial C}{\partial t} = D_{mr}\left(\dfrac{\partial^2 C}{\partial r^2} + \dfrac{1}{r}\dfrac{\partial C}{\partial r}\right) + D_{ma}\dfrac{\partial^2 C}{\partial z^2} - w(r)\dfrac{\partial C}{\partial z} \\ C(r,z,0) = 0 \\ \left.-D_{mr}\dfrac{\partial C}{\partial r}\right|_{r=R} = -\dfrac{1}{2\pi R}\delta(z)\delta(t) + \dfrac{1}{2}vC(R,z,t) \end{cases} \tag{25}$$

where $C(r,z,t)$ is the concentration of solute molecules in the moving zone, C is the abbreviation, D_{ma} and D_{mr} the axial and radial diffusion coefficients in the mobile phase respectively, $w(r)$ the linear flow rate at r, u the mean linear flow rate. In the case of laminar flow, there is

$$w(r) = \frac{2u}{R^2}(R^2 - r^2) \tag{26}$$

Making Fourier–Laplace transform of Eq. (25), we have

$$\begin{cases} D_{mr}\left(\dfrac{d^2\tilde{C}}{dr^2} + \dfrac{1}{r}\dfrac{d\tilde{C}}{dr}\right) + (A_1 - A_2 r^2))\tilde{C} = 0 \\ \left.-D_{mr}\dfrac{d\tilde{C}}{dr}\right|_{r=R} = -\dfrac{1}{2\pi R} + \dfrac{v}{2}\tilde{C}(R,\omega,p) \end{cases} \tag{27}$$

where

$$\begin{cases} A_1 = -D_{ma}\omega^2 + 2iu\omega - p \\ A_2 = \dfrac{2iu\omega}{R^2} \end{cases} \tag{28}$$

The PDF and its transform of the displacement and residence time in the moving zone in an arbitrary step are derived from C and $\tilde{C}$ as follows

$$f_{\eta_m\tau_m}(z,t) = \pi R v C(R,z,t) \tag{29}$$

$$\tilde{f}_{\eta_m\tau_m}(\omega,p)=\pi R v\tilde{C}(R,\omega,p) \tag{30}$$

According to the characteristic function theory of probability, the characteristic function of the sum of independent random variables is equal to the product of the characteristic function of each one. So we have

$$\tilde{f}_{\eta\tau}(\omega,p)=\tilde{f}_{\eta_s\tau_s}(\omega,p)\tilde{f}_{\eta_m\tau_m}(\omega,p) \tag{31}$$

4. Moments of elution curves

Substituting Eq. (31) into Eq. (12) and finding $\omega=\omega(p)$, then substituting $\omega(p)$ into Eq. (13), we finally obtain the Laplace transform of the peak profiles. The nth cumulant of the peak profiles can be derived from the Laplace transform as follows [7,10,14]:

$$M_n'=(-1)^n\frac{\partial^n}{\partial p^n}\ln(\tilde{f}_{\tau_c}(p))\Big|_{p=0}=Lc_n \tag{32}$$

where $M_1'=t_R$, $M_2'=M_2=\sigma_{\tau_c}^2$, $M_3'=M_3$, etc., t_R is the retention time, M_2 or $\sigma_{\tau_c}^2$ are the second central moment or variance of elution curves, M_3 is the third central moment. All the work can be completed by Mathematica, see Appendix B. The results are as follows

$$t_R=(1+k)t_m \tag{33}$$

$$M_2=\left(\frac{2(1+k)^2(D_{ma}+\beta D_{sa})}{u^2}+\frac{(1+6k+11k^2)R^2}{24D_{mr}}+\frac{k^2Rd_l}{3\varepsilon D_{sr}}+\frac{2k'}{\widetilde{k_d}}\right)\times t_m \tag{34}$$

$$M_3=\left(\frac{12(1+k)^3(D_{ma}+\beta D_{sa})^2}{u^4}+\frac{1+k}{u^2}\left(\frac{2kRd_l(kD_{ma}+(1+2k)\beta D_{sa})}{\varepsilon D_{sr}}+\frac{R^2((1+5k+7k^2)D_{ma}+(2+10k+11k^2)\beta D_{sa})}{2D_{mr}}+\frac{12k'(D_{ma}+\beta D_{sa})}{\widetilde{k_d}}\right)+\frac{(3+37k+165k^2+251k^3)R^4}{960D_{mr}^2}+\frac{(3+11k)R^2}{4D_{mr}}\left(\frac{k^2Rd_l}{6\varepsilon D_{sr}}+\frac{k'}{\widetilde{k_d}}\right)+\frac{k^3R^2d_l^2}{5\varepsilon^2D_{sr}^2}+\frac{2kk'Rd_l}{\varepsilon D_{sr}\widetilde{k_d}}+\frac{6k'}{\widetilde{k_d^2}}\right)t_m \tag{35}$$

$$H=\frac{2(D_{ma}+\beta D_{sa})}{u}+\frac{u}{(1+k)^2}\left(\frac{(1+6k+11k^2)R^2}{24D_{mr}}+\frac{k^2Rd_l}{3\varepsilon D_{sr}}+\frac{2k'}{\widetilde{k_d}}\right) \tag{36}$$

where t_m is the time for the fluid to pass through the column, H the theoretical plate height, β the ratio of the pore volume in the static zone to that in the moving zone, k' the ratio of solute amount adsorbed by solid surfaces in the static zone to that in the moving zone, and we call it the adjusted retention factor, k the ratio of solute amount in the static zone to that in the moving zone and called as the retention factor, $\widetilde{k_d^i}$ special average of k_{dj}^i, they are calculated as follows

$$\begin{cases}\beta=\dfrac{d_l}{R^2}(2R+d_l)\varepsilon\\ k'=\beta\varepsilon_s K\\ k=k'+\beta\\ \widetilde{k_d^i}=\left(\dfrac{1}{K}\displaystyle\sum_j\frac{K_j}{k_{dj}^i}\right)^{-1}\end{cases} \tag{37}$$

where K_j is the distribution constant on site j, K is the total distribution constant.

$$\begin{cases}K_j=\dfrac{k'_{aj}}{k_{dj}}\\ K=\displaystyle\sum_j K_j\end{cases} \tag{38}$$

5. Elution curves

In principle the expression of elution curves can be obtained by inverse transform of Eq. (13) with respect to p. However, only in the simplest case, i.e. the all diffusions can be ignored and the surface is of single-site, we can obtain the analytical expression. In this case, we have

$$\tilde{f}_{\eta\tau}(\omega,p)=1+\frac{1}{v}\left(\frac{R(2A_1-A_2R^2)}{2}+\frac{\varepsilon Ad_l(2R+d_l)}{R}\right) \tag{39}$$

where A, A_1 and A_2 are determined by Eqs. (21) and (28) with $D_{sa}=0$ and $D_{ma}=0$. In this way, the Laplace transform is

$$\tilde{f}_{\tau_c}(p)=e^{-k'k_dt_m-pt_m+((k'k_d^2t_m)/(p+k_d))} \tag{40}$$

Making inverse transformation of Eq. (40), we have

$$f(t)=e^{-n-k_d(t-t'_m)}\left(\frac{k_d\sqrt{k't_m}}{\sqrt{t-t'_m}}I_1(2k_d\sqrt{(t_R-t'_m)(t-t'_m)})+\delta(t-t'_m)\right) \tag{41}$$

where $n=k'k_dt_m$ represents the mean times of solute molecules being adsorbed by sites during their passage through the column, $t'_m=(1+\beta)t_m$ the mean time for unretained material to pass through the column, $I_1(x)$ the modified Bessel function of the first kind. Except for the term of $\delta(t-t')$, Eq. (41) is identical to the formula derived by Giddings and Eyring completely [1].

If ignoring merely the radial diffusions, similarly to derivation of Eq. (40), we can derive the Laplace transform of elution curves as follows

$$\tilde{f}_{\tau_c}(p)=e^{N_d\left(1-\sqrt{1+(2p/N_d)(t'_m+n\sum_j((p_{aj}\tau_{sj})/(1+p\tau_{sj})))}\right)} \tag{42}$$

where $N_d=Lu/(2D_a)$, $D_a=D_{ma}+\beta D_{sa}$, $p_{aj}=k'_{aj}/k'_a$, $k'_a=\displaystyle\sum_j k'_{aj}$, $\tau_{sj}=1/k_{dj}$. After replacing the variable p by $-i\omega$, Eq. (42) becomes the same as that of Ref. [5] formally, but here the D_a contains the axial diffusion in the static zone and the effects of multiple-sites have been added.

Once taking into account the radial diffusions, we are not able to obtain an analytical solution of ω from $\tilde{f}_{\eta\tau}(\omega,p)=1$, thereby not able to give an accurate Laplace transform of elution curves, instead we can give an approximate or numerical Laplace transform only. No matter whether the radial diffusions can be ignored or not, except for Eq. (41) we are not able to give an expression of elution curves by inverse transform. For all cases a general method to obtain the elution curves is the numerical calculation by following formula

$$f(t_n)=\frac{\Delta p}{\pi}Re\left(\sum_{j=1}^{j_{\max}}e^{-i\omega(p_j)L+p_jt_n}+0.5\right) \tag{43}$$

where Δp is real-number step size, $p_j=-i\,(j-1)\,\Delta p$, t_n is the nth set value of t for calculating $f(t)$. The calculation of Eq. (43) can be completed by Mathematica, see Appendix C.

6. Effect of pressure drop and extracolumn

There are many papers in the literature discussed the effects of pressure drop and extracolumn on the second moment and the the-

oretical plate height [19–24]. For compressible fluid, the pressure at z in a column can be expressed by

$$P(z) = \sqrt{P_{in}^2 - \frac{(P_{in}^2 - P_{out}^2)z}{L}} \tag{44}$$

The pressure drop will cause change of linear flow rate and diffusion coefficient as follows:

$$u(z) = \frac{u_{out}P_{out}}{P(z)} \tag{45}$$

$$D_m(z) = D_{out}\frac{P_{out}}{P(z)} \tag{46}$$

where P_{out}, u_{out} and D_{out} denote the pressure, mean velocity and diffusion coefficient at the outlet, P_{in} the inlet pressure, $P(z)$, $D_m(z)$ and $u(z)$ are the pressure, mean velocity and diffusion coefficient at z. In case the performance of columns varies with position z, the coefficients c_n in Eq. (B4) become functions of z, and instead of Eq. (B4) the moments need to calculate by integration:

$$M_n' = \int_0^L c_n dz \tag{47}$$

In order to calculate the elution curves with consideration of column-performance change, we divide the column into many short pieces so that the performance in each piece keeps unchanged and Eq. (1) holds true. In this way, for the jth piece, we have

$$\tilde{f}_{j\tau_c}(p) = e^{-i\omega_j(p)\Delta z_j} \tag{48}$$

where ω_j denotes the ω in piece j, Δz_j is the piece length. For the whole column, there is

$$\tilde{f}_{\tau_c}(p) = e^{-i\sum_j \omega_j(p)\Delta z_j} = e^{-i\int_0^L \omega(p)dz} = e^{-i\tilde{\omega}(p)L} \tag{49}$$

where

$$\tilde{\omega}(p) = \int_0^L \frac{\omega(p)}{L}dz \tag{50}$$

There are many types of time distribution of sample injection [23]. Here we only take the following as an example:

$$f_{in}(t) = \begin{cases} \dfrac{1}{t_{in}} & 0 \le t \le t_{in} \\ 0 & t > t_{in} \end{cases} \tag{51}$$

where t_{in} denotes the width of injection time. The Laplace transform of $f_{in}(t)$ is

$$\widetilde{f_{in}}(p) = \frac{1}{pt_{in}}(1 - e^{-pt_{in}}) \tag{52}$$

Suppose that the additional residence time from the extracolumn effects except the sample injection is of a Gaussian distribution with variance σ_{ex}^2, then the Laplace transform of elution curves needs to multiply by a factor of $\exp(\sigma_{ex}^2 p^2/2)$.

With consideration of column-performance change, injection function and the other extracolumn factors, the equation of numerical inverse transform, Eq. (43), needs to be replaced by

$$f(t_n) = \frac{\Delta p}{\pi} Re\left(\sum_{j=1}^{j_{max}} \widetilde{f_{in}}(p_j) e^{(\sigma_{ex}^2 p_j^2/2) - i\tilde{\omega}(p_j)L} - 0.5\right) \tag{53}$$

7. Discussion

The famous equation of theoretical plate height H for capillary porous-layer partition chromatography derived by Golay [15] is

$$H = \frac{2D_m}{u} + \frac{1}{24}\left(\frac{1 + 6k_G + 11k_G^2}{(1+k_G)^2} + \frac{8 + 32k_G}{(1+k_G)^2}\alpha_2 + \frac{8k_G^2}{(1+k_G)^2}\frac{\alpha_1^2}{\alpha_2}\right) \times \frac{R^2 u}{D_m} + \frac{k_G^3}{6(1+k_G)^2}\frac{(1+2\alpha_2)}{F^2K^2}\frac{R^2u}{D_l} \tag{54}$$

where k_G denotes the retention factor defined in Golay's equation, which is slightly different from k in this paper, $k = 2\alpha_2 + (1 + 2\alpha_2)k_G$, $\alpha_1 R$ represents the mean length of a tortuous path, α_2 is equal to the product of ε and δ_1, where $\delta_l = d_l/R$, F is the ratio of the total surface area in the porous layer to the surface area of the moving zone. Substantially, the sum of the second and third terms in Eq. (54) is equal to $(1 + 6k + 11k^2)R^2u/24(1+k)^2D_m$, which can be proved if we substitute k for k_G and expand it in series of α_2. Supposing the orientation of the paths is isotropic, the mean value of $\alpha_1^2R^2$ will approach to 3 d_l^2. So the fourth term in Eq. (54), $k_G^2\alpha_1^2R^2u/3(1+k_G)^2\alpha_2 D_m$, can be deduced to $k_G^2 d_l^2 u/(1+k_G)^2\varepsilon D_m\delta_1$. When $\delta_1 \ll 1$, k_G and k are nearly equal. Replacing k_G by k and $D_m/3$ by D_{sr}, the fourth term can further be deduced to $k^2Rd_lu/3(1+k)^2\varepsilon D_{sr}$. At last, according to the definition of F and K, there is $FK = k_G(1 + 2a_2)R/2d_l$. Substituting the expressions of FK into the last term of Eq. (54) and considering that $k_G \approx k \approx k'$, this term can be simplified to $2k'd_f^2u/3(1+k)^2D_l$. In this way, the Golay equation of Eq. (54) can be rewritten in the symbols of this paper as follows

$$H = \frac{2D_m}{u} + \frac{u}{(1+k)^2}\left(\frac{1 + 6k + 11k^2)R^2}{24D_m} + \frac{k^2Rd_l}{3\varepsilon D_{sr}} + \frac{2k'd_f^2}{3D_l}\right) \tag{55}$$

Comparing Eq. (55) with Eq. (36), we find that all terms of Eq. (55) except the last one are contained in Eq. (36). The exceptive term is brought from the diffusions in the liquid films on solid surfaces, and in this paper we only study the adsorption chromatography in which there are no liquid films, so Eq. (36) does not have this term. By the way, if to use the model of this paper in the partition chromatography, this term appears at once. But the derivation is complex and beyond the scope of this paper. Any way, Eq. (55) lacks the terms corresponding to the axial diffusions in porous layer, $2\beta D_{sa}/u$, and the reaction rate term, $2k'u/(1+k)^2\widetilde{k_d}$.

The moment expressions from CF method of stochastic theory, rewritten by the symbols of this paper, are as follows:

$$M_2 = t_m\left(\frac{2\,D_m(1+k')^2}{u^2} + \frac{2k'}{\widetilde{k_d}}\right) \tag{56}$$

$$M_3 = t_m\left(\frac{12D_m^2(1+k')^3}{u^4} + \frac{12D_mk'(1+k')}{u^2k_d} + \frac{6k'}{\widetilde{k_d^2}}\right) \tag{57}$$

Here we add the effects of multiple-sites in the results of Ref. [5]. Compared with Eqs. (34) and (35), we find that Eqs. (56) and (57) lack the terms related to the radial diffusions in the moving zone and all diffusions in the static zone.

Letting $d_l \to 0$, the moment expressions of Eqs. (34)–(36) become the same as the previous results of ours [11].

According to theory of gas adsorption [16], the number of molecules striking a unit area of solid surface in unit time is $vC/4$, where C represents the molar concentration near the surface. Suppose that total active surface, i.e. the surface occupied by all active sites, has a portion P_a in the total surface and the reflection coefficient on the site is α, in equilibrium we have

$$\frac{v(1-\alpha)P_a}{4}C = k_dC_s \tag{58}$$

where

$$k_d = \frac{1}{\tau_0}e^{-Q/(RT)} \tag{59}$$

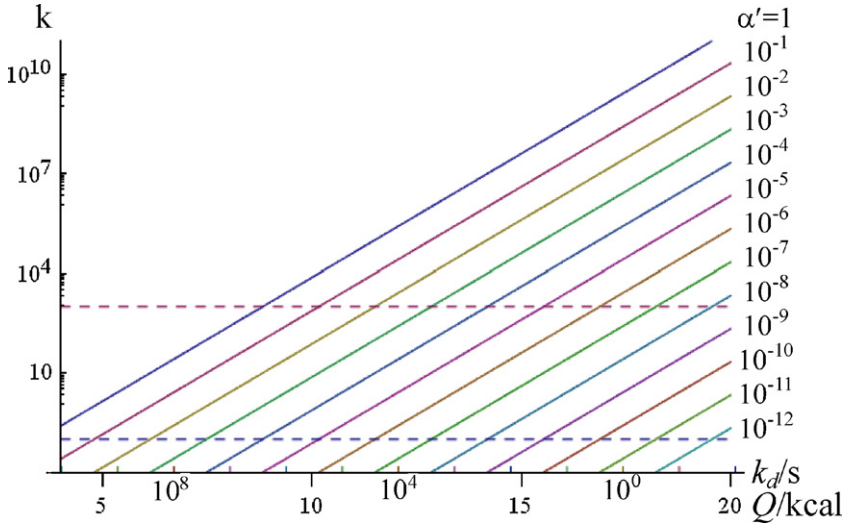

Fig. 2. The relationship of retention factors, adsorption heat and condensation coefficients. $\delta_1 = 0.2$, $\varepsilon = 0.6$, $\varepsilon_s = 10^6$/cm, $v = 400$ m/s, $T = 293$ K.

From Eqs. (58) and (59),

$$K = \frac{C_s}{C} = \frac{1}{4}v\alpha'\tau_0 e^{-Q/(RT)} = \frac{k'_a}{k_d} \tag{60}$$

where

$$\alpha' = (1-\alpha)P_a \tag{61}$$

$$k'_a = \frac{1}{4}v\alpha' \tag{62}$$

Q is the molar adsorption heat, R the gas constant, T the Kelvin temperature, τ_0 the oscillation time of adsorbed molecules, $\tau_0 \approx 10^{-13}s$, α' is the condensation coefficient. Substituting K into Eq. (37), we have

$$k' = \frac{1}{4}v\alpha'\beta\varepsilon_s\tau_0 e^{-Q/(RT)} = \frac{1}{4k_d}v\alpha'\beta\varepsilon_s \tag{63}$$

From above equation it can be seen that for constant α', the smaller the k_d, the larger the k'. In other words, the larger the Q, the larger the k'.

Fig. 2 gives an intuitionistic numerical relationship of k' and Q. In Fig. 2, the two dashed level lines correspond to $k' = 1000$ and $k' = 0.1$, respectively. Generally, that k' falls outside the two lines is not suitable for analysis. Hence when the Q is very large, the α' must be very small in order to make k' falling inside the two lines. α' may decrease, for example, by adding some inert surfaces to reduce P_a. Besides α', the factors of δ_1, ε, ε_s and v, etc. can also affect the value of k', especially the factor of ε_s can affects k' by several orders of magnitude.

Fig. 3 gives the relations of the theoretical plate height and the desorption rate constant with given k'. In the figure three kinds of curves, by CF method, i.e. from Eq. (56), Golay equation, i.e. from Eq. (55) with $d_f = 0$, and this paper, i.e. Eq. (36), are simultaneously plotted. From the figure we can find that the relations from CF method and Golay equation are entirely different. CF method is suitable for small k_d, in which desorption rate is the controlling factor, and Golay equation is suitable for large k_d, in which diffusion is the controlling factor [17]. And the results of this paper coincide with that from CF method completely when k_d is very small and coincide with that from Golay equation when k_d is very large. This shows that the model of this paper is suitable for both cases of small k_d and large k_d, and combines the both effects of diffusions and desorptions into a united equation. From Fig. 3 it also seen that H calculated by this paper and Golay equation decreases with increasing of D_m. But the results by CF method are just the reverse. This is because that the radial diffusions are neglected here and under the given conditions the effects of radial diffusions are lager than axial diffusions. Fig. 3 also shows the relations of H and Q because Q and k_d are of one-to-one correspondence.

Skew is defined as

$$S = \frac{M_3}{M_2^{3/2}} \tag{64}$$

where S represents the skew. Fig. 4 shows the relations of skew to adsorption heat and desorption rate constants for the single-site model. From this figure it is seen that skew increases with decreasing of k_d and k' when k' is not extremely small, but suddenly becomes quite small when k' is close to 0. This means that skew increases first then decreases with k' increasing from $k' = 0$. For small k_d and small but not zero k', skew becomes very large. But for sufficiently large k_d, in despite of the value of k', the skew is always small.

In the case of multiple-site, suppose the adsorption heat of site j is Q_j and the desorption rate constant is k_{dj}, then

$$k_{dj} = \frac{1}{\tau_0}e^{-Q_j/(RT)} \tag{65}$$

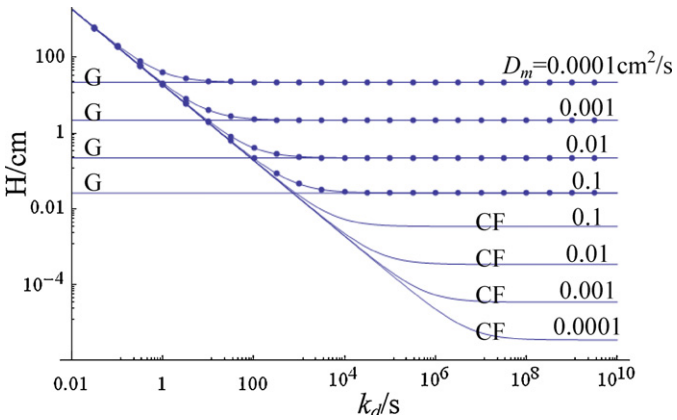

Fig. 3. The relation of H to D_m and k_d. G means the curves are calculated by Golay equation, CF by characteristic function of stochastic theory, the dots by this paper. $L = 20$ m, $R = 0.01$ cm, $u = 50$ cm/s, $k' = 2$, $\beta = 0.264$.

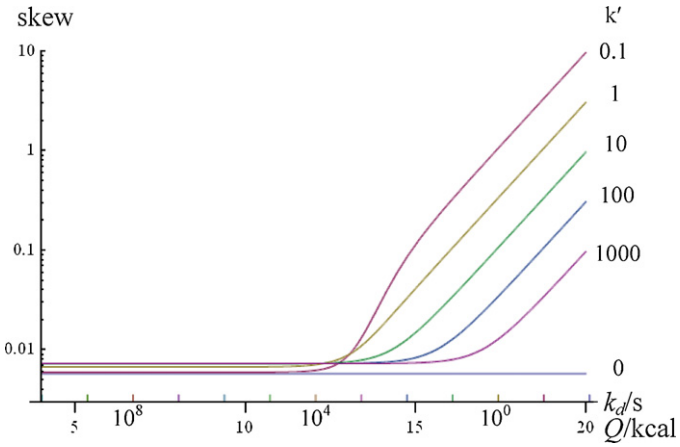

Fig. 4. The relation of skew and adsorption heat for single-site. $L = 20$ m, $R = 0.01$ cm, $u = 50$ cm/s, $D_m = 0.1$ cm^2/s, $\delta_1 = 0.2$, $\varepsilon = 0.6$, $\varepsilon_s = 10^6$/cm, $v = 400$ m/s, $T = 293$ K.

From the principle of chemical equilibrium, we have

$$\frac{v(1-\alpha_j)P_aP_j}{4}C = k_{dj}C_{sj} \tag{66}$$

From Eq. (66),

$$k'_{aj} = \frac{1}{4}v(1-\alpha_j)P_aP_j = \frac{1}{4}v\alpha'_jP_j \tag{67}$$

where P_j is the abundance of site j, equal to the ratio of surface area occupied by this site to that by all sites, α_j is the reflection coefficient on site j, $\alpha'_j = (1-\alpha_j)P_a$ is the condensation coefficient. Substitute above k_{dj} and k'_{aj} into Eqs. (37) and (38), then re-substituting the results into Eqs. (33)–(36) and (64), we can obtain the retention factors, the retention time, the theoretical plate height and the skew, etc. for different Q_j. Introducing k'_j into the expressions of the moments,

$$k'_j = \frac{1}{4}v\alpha'_j\beta\varepsilon_s\tau_0 e^{Q_j/(RT)} \tag{68}$$

where k'_j represents the adjusted retention factor of site j, we can obtain the moments for different k'_j.

Fig. 5 gives the intuitionistic relations of skew to abundance P_2 in two-site case under different k'_1 and k'_2. From this figure it is seen that all curves of skew vs. P_2 are similar, they all increase first and then decrease with increasing of P_2 and reach a peak value at a small P_2. For given k_{d2} the curves shift to the left integrally as k'_2

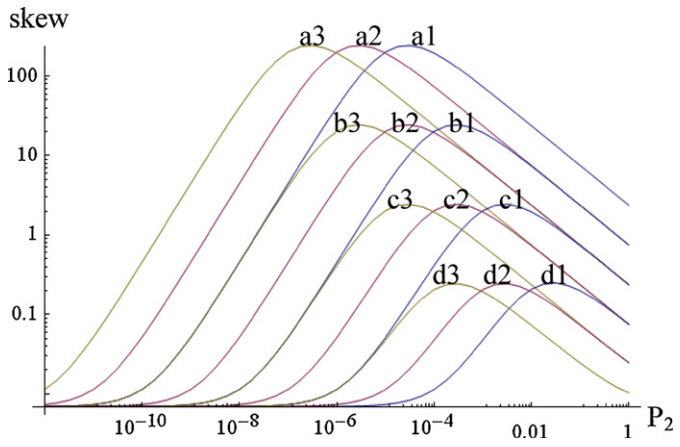

Fig. 5. The relation of skew and abundance for two-site. $k'_1 = 2$, $k_{d1} = 10^8$/s. (a) $k_{d2} = 0.01$/s, (b) $k_{d2} = 0.1$/s, (c) $k_{d2} = 1$/s, (d) $k_{d2} = 10$/s, 1. $k'_2 = 2$, 2. $k'_2 = 20$, 3. $k'_2 = 200$. The other parameters see Fig 4.

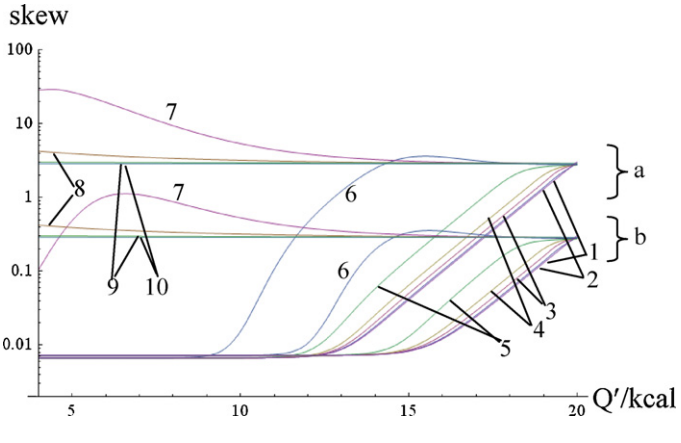

Fig. 6. Relation of skew to adsorption heat distribution. $\alpha'(Q) =$ constant for each curve. $Q_1 = 4$ kcal, $Q_2 = 20$ kcal, 1. $\sigma_Q = 0$ kcal, 2. $\sigma_Q = 0.1$, 3. $\sigma_Q = 0.2$, 4. $\sigma_Q = 0.3$, 5. $\sigma_Q = 0.5$, 6. $\sigma_Q = 1$, 7. $\sigma_Q = 2$, 8. $\sigma_Q = 3$, 9. $\sigma_Q = 5$, 10. $\sigma_Q = 100$, (a) $k' = 1$, (b) $k' = 100$. The other parameters are same as in Fig 4.

increases. For given k'_2, as k_{d2} decreases, the peak values of skew-P_2 curves increase and even get very large. These plots are analogous to those of Ref. [4] qualitatively.

In the case of continuously distributed sites, α' and k_d are related to the adsorption heat Q, and the calculation of K and k_d^i should be replaced by integration:

$$K(Q) = \frac{k'_a(Q)}{k_d(Q)} = \frac{v}{4}\tau_0 e^{Q/(RT)}\alpha'(Q)P(Q) \tag{69}$$

$$K = \frac{v}{4}\tau_0 \int e^{Q/(RT)}\alpha'(Q)P(Q)dQ \tag{70}$$

$$\widetilde{k_d^i} = \left(\frac{1}{K}\int \frac{K(Q)}{k_d^i(Q)}P(Q)dQ\right)^{-1} = \frac{\int \alpha'(Q)P(Q)/k_d(Q)dQ}{\int \alpha'(Q)P(Q)/k_d^{i+1}(Q)dQ} \tag{71}$$

where $\alpha'(Q)$ denotes the condensation coefficient on the site with adsorption heat of Q, $P(Q)dQ$ represents the abundance of the site with adsorption heat in $(Q, Q+dQ)$,

$$\alpha'(Q) = (1-\alpha(Q))P_a \tag{72}$$

where $\alpha(Q)$ is the reflection coefficient on the site with adsorption heat Q. In the case of continuous distribution, the relation of elution-curve moments to adsorption heat is very complex. It is not only related to adsorption heat distribution $P(Q)$, but also to $\alpha'(Q)$. Fig. 6 gives the relations between skew and the parameters of distribution under the conditions $\alpha'(Q) = const$ and

$$P(Q) = \begin{cases} e^{-(Q-Q')^2/2\sigma_Q^2} & Q_1 \le Q < Q_2 \\ 0 \quad Q < Q_1 & \text{or} \quad Q \ge Q_2 \end{cases} \tag{73}$$

In the figure, curves 1, 2 and 3 almost coincide completely with each other. Curve 1 just corresponds to single-site case. So above curves show that the surface with continuous distribution of $\sigma_Q < 0.2$ kcal can be considered as uniform. In the region of $\sigma_Q < 0.5$ kcal skew monotonously increases with Q'. When σ_Q is between 0.5 kcal and 3 kcal, skew increases first and then decreases with increasing of Q'. When σ_Q reaches a very large value, the adsorption heat distribution turns to uniform, and skew becomes independent of Q'. For given smaller Q' skew varies sensitively with σ_Q, for example, at $Q' = 7$ kcal and $k' = 1$, $\sigma_Q = 0.5$ kcal leads to skew = 0.0067, $\sigma_Q = 2$ kcal leads to skew = 13.4 and $\sigma_Q = 3$ kcal leads to skew = 3.5. The curves of different k' are similar, but larger k' gives smaller skew.

Fig. 7 gives several elution curves of single-site model. From this figure we find that curves 1, 2 and 3 are all split to two parts: a

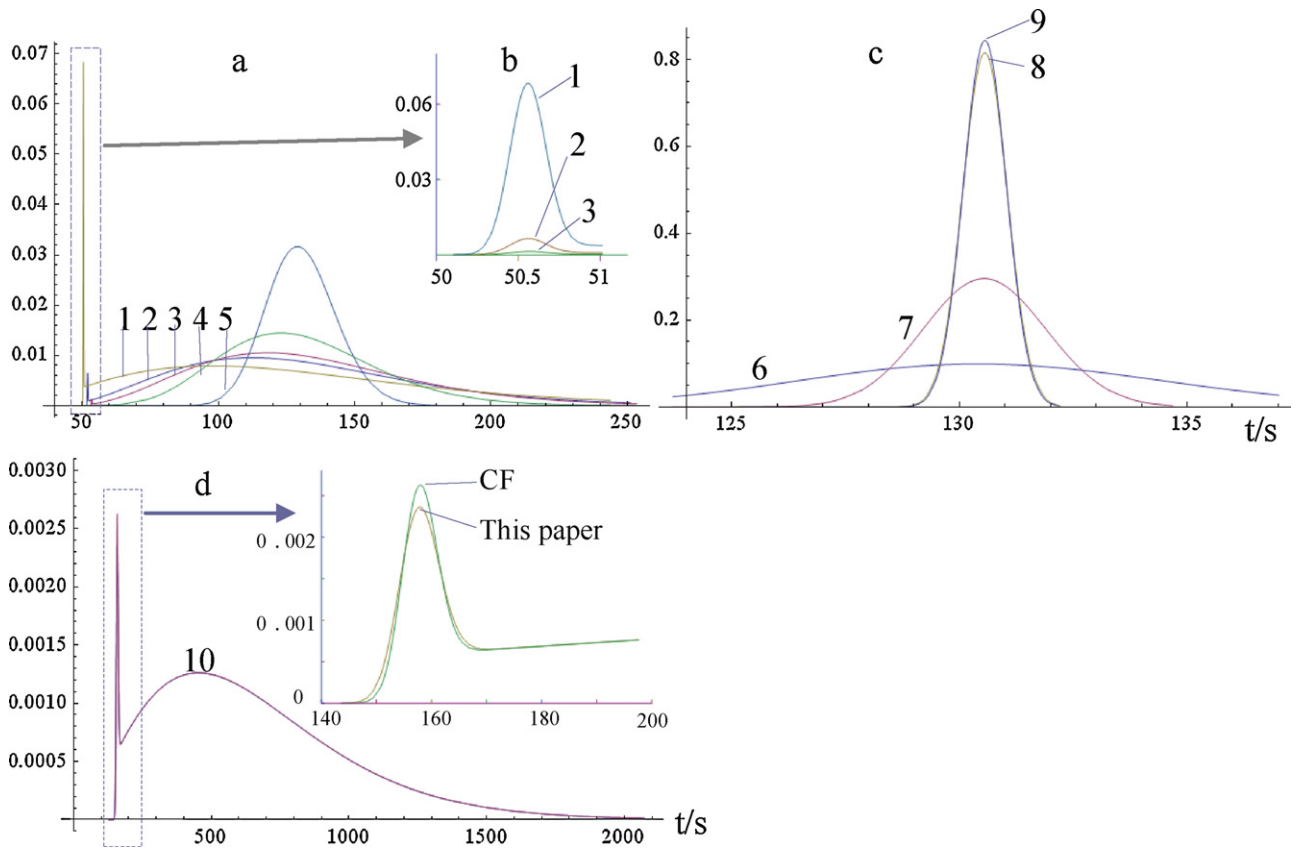

Fig. 7. Elution curves for single-site model. 1. $k_d = 0.05$/s, skew = 1.06, $n = 4$; 2. $k_d = 0.08$/s, skew = 0.84, $n = 6.4$; 3. $k_d = 0.1$/s, skew = 0.75, $n = 8$; 4. $k_d = 0.2$/s, skew = 0.53, $n = 16$; 5. $k_d = 1$/s, skew = 0.24, $n = 80$; 6. $k_d = 10$/s, skew = 0.075, $n = 800$; 7. $k_d = 100$/s, skew = 0.024, $n = 8 \times 10^3$; 8. $k_d = 10^4$/s, skew = 0.0072, $n = 8 \times 10^5$; 9. $k_d = 10^6$/s, skew = 0.0069, $n = 8 \times 10^7$. 10. $L = 25$ cm, $u = 0.2$ cm/s, $D_m = 10^{-3}$ cm^2/s, $k_d = 0.008$/s, $k' = 4$. For curves 1–9, $k' = 2$. The other parameters are same as Fig. 4.

sharp peak, corresponding to unretained molecules, and a short fat peak, corresponding to retained molecules. This phenomenon was reviewed in ref. [18]. Note, the three unretained peaks are located at the same position originally, for clarity we move curves 2 and 3 to right a bit. From curves 1–9, the corresponding k_d increases from 0.05/s to 10^6/s. As k_d increases, the unretained peaks become smaller and smaller and the retained peaks become higher and higher, narrower and narrower, at last, for slightly large k_d the unretained peak disappears completely, leaving the retained peak alone and for very large k_d the retained peak becomes independent of k_d. Actually, an elution curve is split or not is controlled mainly by the mean times of being adsorbed, which is denoted by n, $n = k'k_d t_m$. The probability that a molecule is never adsorbed during the course of passing through the column can be calculated by e^{-n}. So for large n, the probability tends to 0 and the unretained peak disappears. And for small n, the probability tends to 1 and the retained peak disappears. Besides n, the splitting is also controlled by the difference of position of the two peaks and by the width of slow peak. From Fig. 4 it has been seen that when k' and k_d both are small, the skew will be very large. But the large skew is only a theoretical value calculated from whole elution curve, and in practice, in this case the n is very small, and the observed curve is an unretained profile and has good symmetry with small skew. The characteristic of elution curves for single-site model stated here

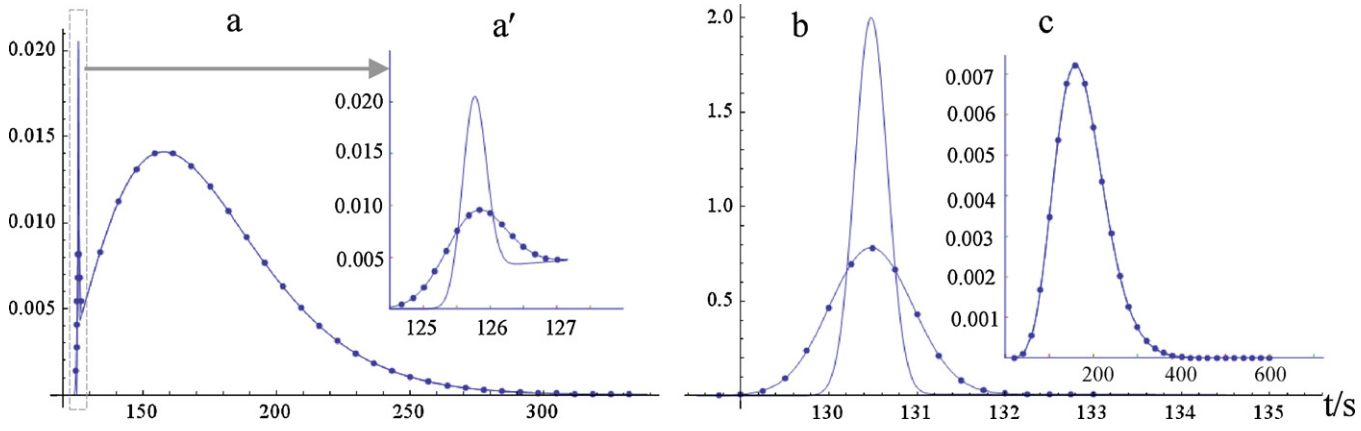

Fig. 8. Elution curves for two-site model. The curves with dots are given by Eq. (55), the curves without dots are by CF method [4,5]. $k'_1 = 2$, $k'_2 = 20$, $k_{d1} = 10^8$/s, $k_{d2} = 0.1$/s. (a) $P_2 = 0.06$, skew = 0.97, $n = 4.8$; (b) $P_2 = 0.001$, skew = 7.3, $n = 0.08$; (c) $P_2 = 0.2$, skew = 0.53, $n = 16$. The other parameters are same as Fig. 4.

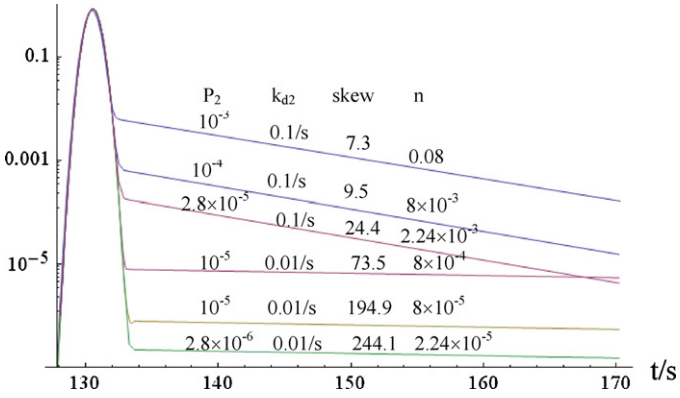

Fig. 9. Tailing caused by minor slow-site. $k'_1 = 2$, $k'_2 = 20$, $k_{d1} = 10^8$/s, the other parameters see Fig. 4.

is similar to Ref. [4]. However, because of neglecting radial diffusions the unretained peak plotted by CF method will be higher and narrower. This can be shown by curves 10, the parameters of which are specially set as the same as Fig. 3 of Ref. [4]. The retained peaks by CF method and this paper are not different because in the case of small k_d they are less affected by the parameters other than k_d.

Fig. 8 shows the varying of two-site elution curves with abundance of site 2. The curves in Fig. 8 are calculated by two methods: Eq. (42) with $D_{sa} = 0$, corresponding to CF method [3,5], and Eq. (43) of this paper. The curves with dots are calculated by Eq. (43) and the curves without dots are by CF method. In Fig. 8a, an elution curve is split to two peaks: the first peak corresponds to the sites with large k_d and is unretained by the sites with small k_d, which we can call a quick peak, and the second peak is retained by the slow-site, which can be called a slow peak. In Fig. 8b there are only the quick peaks, and in Fig. 8c there are only the slow peaks. Similarly to the single-site case, whether an elution curve is split or not is also determined mainly by n, here $n = P_2 k'_2 k_{d2} t_m$ and represents the mean times of being adsorbed by the slow-sites. In Fig. 8a, $n = 4.8$, the probability of unretained by slow-sites is 0.82%. i.e. the area of the quick-site peak is 0.82% in the total area of the elution curve. Although the portion is small, the peak is very distinct because it is very narrow. In Fig. 8b, $n = 0.08$, the portion of the quick-site peak is 92.3%. Although the slow-site profile or tailing has a portion still as much as 7.7%, it disappears completely because it spreads too broadly. In Fig. 8c, $n = 16$, the portion of the quick-site peak decreases to 10^{-7} and the whole elution curve is controlled by slow-sites completely. By comparison of the results of the two methods it can be found that the quick-site peaks calculated by this paper are fatter and shorter than those by CF method, and the slow-site peaks are not different. The reason for this is similar to that for single-site case, i.e. in the CF method the radial diffusions are neglected.

Fig. 9 further illustrates the influence of minor slow-sites on elution curves. From this figure it is seen that a small amount of slow-sites causes a long tailing. As the abundance of slow-sites decreases the tailing descends also, but the decay rate of the tailing is unchanged, basically equal to k_{d2}. It is also seen that for very small P_2 and k_{d2}, the tailing becomes very low, and the corresponding skew becomes very large. However, the small tailing can be observed only in semilog plot theoretically and in practice it may be drowned by noise entirely.

Fig. 10 gives the curves with continuously distributed adsorption heat. From this figure we can see that the curve 2, whose σ_Q is 1 kcal, is completely identical to the curve with $\sigma_Q = 0$ kcal, i.e. the case of single-sites. This means that the elution curves with continuously distributed adsorption heat have no significant difference from that of single-sites provided σ_Q is not too large. From curve 2 to curve 8, σ_Q is from 0 kcal to 100 kcal, the peak symmetry becomes worse and worse. It is interesting that in the figure curve 4 has the maximum skew of 13.2, but it does not look the worst symmetrical, and curve 8 looks have the worst symmetry, but its skew is 2, not the biggest. Comparing curves 8, 9 and 10, we find that under the condition of $\sigma_Q = 100$ kcal, with k' increasing the skew decreases and the symmetry increases.

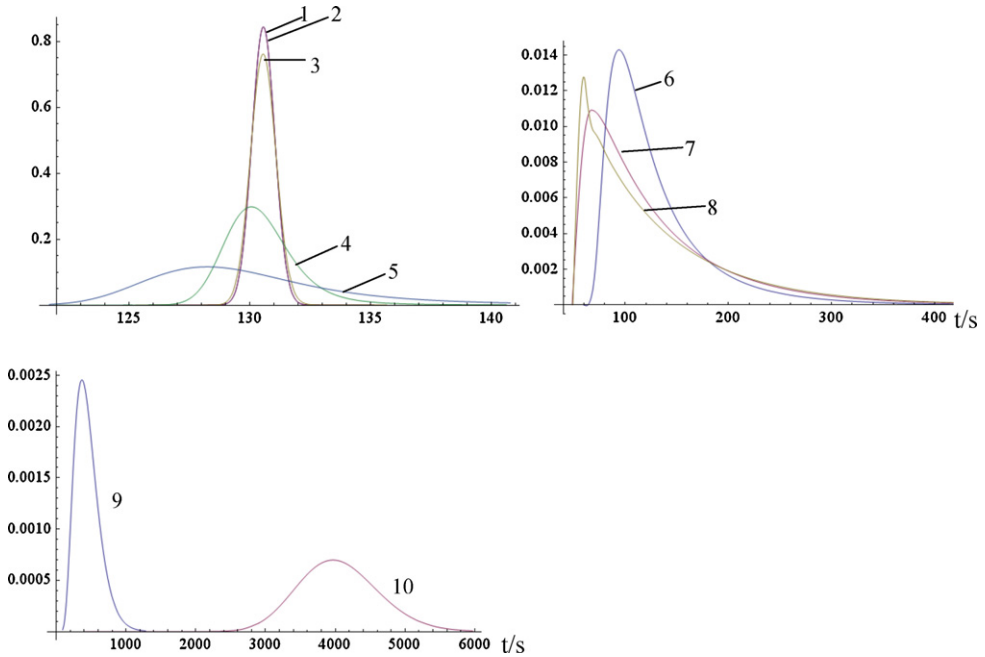

Fig. 10. Elution curves for continuously distributed adsorption heat. $\alpha'(Q)$ = constant for each curve. $Q_1 = 4$ kcal, $Q_2 = 20$ kcal, $Q' = 7$ kcal, $k' = 2$ except curves 9 and 10; 1. $\sigma_Q = 0$ kcal, skew = 0.0069; 2. $\sigma_Q = 1$, skew = 0.0069; 3. $\sigma_Q = 1.5$, skew = 0.26; 4. $\sigma_Q = 1.8$, skew = 13.2; 5. $\sigma_Q = 2$, skew = 9.43; 6. $\sigma_Q = 3$, skew = 2.49; 7. $\sigma_Q = 5$, skew = 2.11; 8. $\sigma_Q = 100$, skew = 2.03; 9. $\sigma_Q = 100$, $k' = 10$, skew = 0.92; 10. $\sigma_Q = 100$, $k' = 100$, skew = 0.29. The other parameters see Fig. 4.

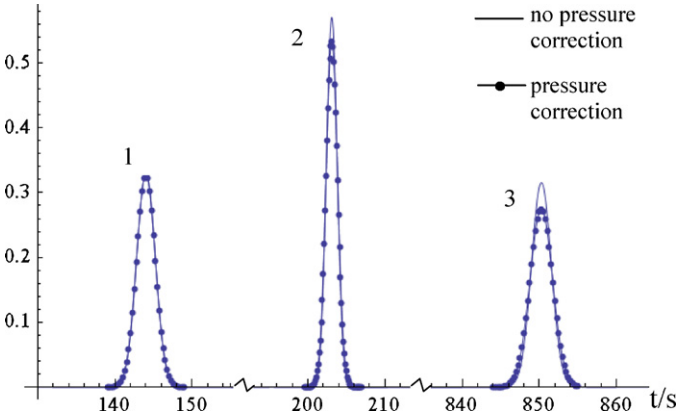

Fig. 11. The effect of pressure change. u_{out} = 50 cm/s; D_{out} = 0.1 cm^2/s; P_{out} = 1 atm, 1. P_{in} = 1.2 atm, R = 0.025 cm, t_m = 44s; 2. P_{in} = 2, R = 0.01, t_m = 62; 3. P_{in} = 7.7, R = 0.005, t_m = 260. The other parameters see Fig. 4.

Fig. 11 shows the effect of pressure drop on elution curves in gas adsorption chromatography. In the figure, the label of no pressure correction means the linear velocity of fluid and the diffusion coefficient both correspond to the average pressure $\bar{P} = 2(1 + P_{in} + P_{in}^2)/3(1 + P_{in})$, without regard to their changing with position. In the figure, curve 1 actually contains two coincided curves: one has been corrected for pressure and the other has not. This means that when $P_{in} \leq 1.2$ atm, the pressure correction is not necessary. But when $P_{in} \geq 2$, the peak becomes shorter and fatter after pressure correction, see curves 2 and 3. It is noticed that curve 2 is narrower than curve 1. This is because the column radius of curve 2 is less than that of curve 1, which reduces the contribution to peak width

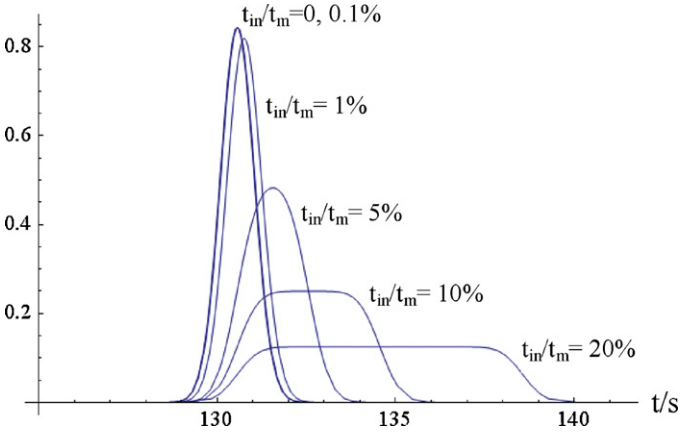

Fig. 12. Effect of injection on elution curves. The calculation conditions are the same as curve 9 of Fig. 7.

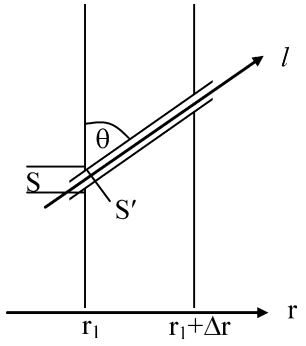

Fig. A1. Schematic of a pore orientation.

of radial diffusions. But the radius of curve 2 is less than that of curve 3 also, this time the curve 2 is broader than curve 3. This is because that the time for fluid to pass through the column of curve 3 is extended greatly and the axial diffusions take effect.

Fig. 12 shows the effect of injection time on elution curves. When the variance from inject time reaches a comparable value with that from Eq. (34), the effect starts to appear. In this figure we can see that the curves with t_{in}/t_m = 0.1% and t_{in}/t_m = 0 are in complete agreement, indicating that injection has no effect on elution curves in this case. Injection time less than or equal to 0.1% of t_m corresponds to length of sample tube less than or equal to about 0.1% of column length. This means, for example, for a column of 20 m long the sample tube up to 2 cm long does not affect the elution curves. When the injection time reaches 1% of t_m, the peak of elution curves is slightly shorter, showing that the injection has a slight effect on the curves. When the injection time exceeds 5% of t_m, elution curves are severely affected and the peaks become fatheaded.

8. Conclusions

In this paper, a set of mass balance equations with special boundary conditions are used to calculate the joint probability density function and the moments of the residence time and the displacement in porous layers in a step, i.e. the step moments and step PDF for the static zone. Again, a similar method is used to obtain the step moments and step PDF for the moving zone. Then probability theory and numerical inversion are used to derive the retention time, the height equivalent to a theoretical plate, the skew and the elution curves from the step moments and the step PDF. By compared with the classic mass balance equation theory and the stochastic theory, the results from this paper are in agreement with those from the two theories in the regions where they hold true separately. From this we can conclude that using mass balance equations to describe the probability distribution of residence time is effective and rigorous and the model of this paper is more general.

The relationship of elution curves and their moments with the step PDF and the step moments is derived only based on probability theory without referring any practical chromatographic models, and it is universal. Therefore as long as we present a set of correct mass balance equations to describe the step probability distributions, we can obtain the elution curves and their moments for any types of linear capillary chromatography in similar way to this paper.

Acknowledgements

The author is grateful to Dr. Haile Lei for his serious correction of the English of this paper. The author is also grateful to Prof. Yibei Fu and Prof. Ying Sun for their support.

Appendix A. Approximate diffusion equation in porous media

Suppose there is a pore of an included angle θ with the radial axis r, see Fig. A1. Set C the solute molecular concentration in pores at r at t, S' the cross section area of the pore, S the section area of the pore cut by the interface of $r = r_1$ and dC/dr the concentration gradient along r direction, then the concentration gradient along the pore axis is $dC/dl = \cos(\theta)dC/dr$. Since $S' = S\cos(\theta)$, we have

$$j = \frac{J}{S} = -D_m \frac{S'}{S}\frac{dC}{dl} = -D_m \cos^2(\theta)\frac{dC}{dr} \tag{A1}$$

where J is the total amount of solute molecules diffusing outwards at the interface r_1 per unit time through the pore l, j is the amount per unit section area of pores per unit time, D_m is the diffusion coefficient of the solute molecules in the mobile media. Suppose

the orientation and cross section area of pores are independent of each other, and the orientations are homogeneously distributed, after averaging over all pores we have

$$j = D_m\overline{\cos^2(\theta)}\frac{dC}{dr} = \frac{D_m}{3}\frac{dC}{dr} \tag{A2}$$

Let

$$D = \frac{D_m}{3} \tag{A3}$$

We have

$$j = -D\frac{dC}{dr} \tag{A4}$$

where D is an equivalent diffusion coefficient. From this it follows that

$$\frac{\partial C}{\partial t} = D\Delta C \tag{A5}$$

Eq. (A5) shows that the diffusion equation in the porous media can be equivalent to the equation in the uniform media, however the diffusion coefficient is an equivalent one.

Appendix B. Derivation of moments

The nth cumulant of an elution curve can be derived from its Laplace transform by Eq. (32). However, $\tilde{f}_{\tau_c}(p)$ is a complicated implicit function of p and its higher-order derivatives are very difficult to calculate even by computing software. Therefore, in order to obtain the moments expediently we would rather first expand $\tilde{f}_{\eta_{s1}\tau_{s1}}(\omega, p)$ in series of d_l and $\tilde{f}_{\eta_m\tau_m}(\omega, p)$ in series of R, then calculate the elution-curve moments by Eq. (32). In order to calculate accurate moments up to order 3, it is necessary to expand $\tilde{f}_{\eta_{s1}\tau_{s1}}(\omega, p)$ in 5th order series of d_l and $\tilde{f}_{\eta_m\tau_m}(\omega, p)$ in 11th order series of R.

From Eqs. (3) and (12), we have

$$\sum_{n=0}^{\infty}\sum_{m=0}^{\infty} M^0_{nm}(\eta, \tau)\frac{(i\omega)^n}{n!}\frac{(-p)^m}{m!} = 1 \tag{B1}$$

where $M^0_{n,m}(\eta, \tau)$ denotes the origin moments of nth order for η and mth order for τ. $M^0_{n,m}(\eta, \tau)$ is given by

$$M^0_{n,m}(\eta, \tau) = i^{-n}(-1)^m \left.\frac{\partial^{n+m}\tilde{f}_{\eta\tau}(\omega, p)}{\partial\omega^n\partial^m p}\right|_{\omega=0,p=0} \tag{B2}$$

Expanding ω in series of p as follows

$$\omega = i\sum_{n=1}^{\infty}\frac{c_n}{n!}(-p)^n \tag{B3}$$

Substituting Eq. (B3) into Eq. (13), then from Eq. (32), we can obtain

$$M'_n = Lc_n \tag{B4}$$

Substituting Eq. (B3) into Eq. (B1) again, we can obtain c_n as follows, $c_1 = M^0_{0,1}(\eta, \tau)/M^0_{1,0}(\eta, \tau)$, $c_2 = (M^0_{0,2}(\eta, \tau) - 2c_1M^0_{1,1}(\eta, \tau) + c_1^2M^0_{2,0}(\eta, \tau))/M^0_{1,0}(\eta, \tau)$, etc. Generally, c_n can be given by the following recurrence formula:

$$\begin{cases} c_n = \dfrac{1}{M^0_{1,0}(\eta, \tau)}\left[M^0_{0,n}(\eta, \tau) - \displaystyle\sum_{k=1}^{n-1} M^0_{1,k}(\eta, \tau)\frac{n!}{(n-k)!k!}c_{n-k} + \sum_{k=2}^{n}\sum_{m=2}^{k}\frac{n!}{m!(k-m)!}M^0_{m,k-m}(\eta, \tau)a_{m,n-k+1}\right] \\ a_{n,m} = -\displaystyle\sum_{j=1}^{m}\frac{1}{j!}a_{n-1,m-j+1}c_j \\ a_{0,m} = \delta(m-1) \end{cases} \tag{B5}$$

where $a_{n,m}$ are intermediate variables, $\delta(m)$ is the discrete δ function. The resulted moments above can be simplified further by change of variables as

$$\sum_j \frac{k'_{aj}}{p + k_{dj}} = \sum_j k'_{aj}\sum_{i=0}\frac{(-p)^i}{k_{dj}^{i+1}}$$

$$= \sum_{i=0}(-p)^i\sum_j\frac{k'_{aj}}{k_{dj}^{i+1}} = K\sum_{i=0}(-p)^i\frac{1}{K}\sum_j\frac{K_j}{k_{dj}^i} = K\sum_{i=0}\frac{(-p)^i}{\widetilde{k_d^i}},$$

where K, K_j and $\widetilde{k_d^i}$ are defined by Eqs. (37) and (38). According to above expression and Eq. (37), Eq. (21) changes to

$$A = -D_{sa}\omega^2 - p\left(1 + \frac{k'}{\beta}\left(1 + \sum_{i=1}\frac{(-p)^i}{\widetilde{k_d^i}}\right)\right) \tag{B6}$$

Eqs. (B2) and (B4)–(B6) are all used in the program for deriving moments.

The program is written in Mathematica of Walfram. In the program, fs, fm, fsm, $M0\eta\tau$(n,m), c[n], a[n, m], kdw[j] and kp represent $\tilde{f}_{\eta_{s1}\tau_{s1}}(\omega, p)$, $\tilde{f}_{\eta_m\tau_m}(\omega, p)$, $\tilde{f}_{\eta\tau}(\omega, p)$, $M^0_{n,m}(\eta, \tau)$, c_n, $a_{n,m}$, $\widetilde{k_d^j}$ and k' correspondingly, the other symbols have the same meaning as in the text, but all subscripts are written in the normal position. $\tilde{f}_{\eta_{s1}\tau_{s1}}(\omega, p)$ and $\tilde{f}_{\eta_m\tau_m}(\omega, p)$ are complex functions of molecular velocity v. However, parameter v plays little role in the ultimate results [11]. To simplify the results, in the program $\tilde{f}_{\eta_{s1}\tau_{s1}}(\omega, p)$ and $\tilde{f}_{\eta_m\tau_m}(\omega, p)$ are expanded in series of $1/v$ and the higher order terms of $1/v$ are omitted.

The program is as follows:

```
(*Solve eq.(20) and find f̃_{η_{s1}τ_{s1}}(ω,p),i.e.fs*)
fs = Normal[Series[π*R*v*y[r] /. DSolve[{Dsr*(y''[r] + 1/r*y'[r])
     + A*y[r] == 0, y'[R + dl] == 0, -Dsr*y'[R] == (1 - π*R*v*y[R])
     / (2*π*R)}, y[r], r][[1]] /. r → R, {v, ∞, 1}]] // Simplify;
(*Solve eq.(28) and find f̃_{η_mτ_m}(ω,p),i.e.fm*)
ym[r_] = y[r] /. DSolve[{Dmr*(y''[r] + 1/r*y'[r]) + (A1 - A2*r^2)*y[r] == 0},
    y[r], r][[1]] /. C[1] → 0;
fm = Normal[Series[π*R*v*ym[R] /. Solve[Dmr*ym'[R] ==
      (1 - π*R*v*ym[R]) / (2*π*R), C[2]][[1]], {v, ∞, 1}]] // Simplify;
(*Expand f̃_{η_{s1}τ_{s1}}(ω,p) and f̃_{η_mτ_m}(ω,p)*)
fs = Normal[Series[fs, {dl, 0, 5}]] // FullSimplify;
fm = Normal[Series[fm, {R, 0, 11}]] // FullSimplify;
(*Construct f̃_{ητ}(ω,p) and omit the terms of higher order power of 1/v*)
fsm = Normal[Series[(ϵ*fs + 1 - ϵ)*fm, {v, ∞, 1}]];
(*Calculate c_m by recurrence algorithm*)
M0ητ[n_, m_] := i^-n*(-1)^m*D[fsm /. {A1 → -Dma*ω^2 + 2*i*u*ω - p,
    A2 → 2*i*u*ω/R^2, A -> -Dsa*ω^2 - p*((k - β)/β (1 + Sum[(-p)^j/kdw[j], {j, 1, m-1}]) + 1)},
    {ω, n}, {p, m}] /. {ω → 0, p → 0};
a[n_, i_] := Which[n == 0, DiscreteDelta[i - 1], n > 0,
 -Sum[a[n - 1, i - j + 1]*c[j]/j!, {j, 1, i}], True, 0];
c[m_] := 1/M0ητ[1, 0]*(M0ητ[0, m] - Sum[m!*M0ητ[1, j]*c[m - j]/(j!*(m - j)!), {j, 1, m-1}] +
  Sum[Sum[(m!*M0ητ[n, j - n]*a[n, m - j + 1])/(n!*(j - n)!), {n, 2, j}], {j, 2, m}]);
(*Calculate the moments*)
Print["tR=", tR = c[1]*L /. L → u*tm /. ϵ → R^2 β/(dl (2 R + dl)) // Simplify];
Print["M2=", M2 = Collect[Normal[Series[c[2] L /. L → u tm /. Dsr → Dar/ϵ
     /. ϵ → R^2 β/(dl (2 R + dl)), {dl, 0, 2}]] /. Dar → Dsr ϵ,
    {tm, u, Dmr, Dsr, kdw}, Factor] /. k - β → kp];
Print["M3=", M3 = Collect[Normal[Series[c[3] L /. L → u tm /. Dsr → Dar/ϵ
     /. ϵ → R^2 β/(dl (2 R + dl)), {dl, 0, 2}]] /. Dar → Dsr ϵ,
    {tm, u, Dmr, Dsr, kdw}, Factor] /. k - β → kp];
Print["H=", Collect[M2*L/tR^2 /. L → tm*u, u]];
```

Appendix C. Numerical inverse Laplace transform

Program of numerical inverse Laplace transform consists of several modules. Modules Basicdata, Basicdata 1 and Basicdata 2 are used to input basic parameters, and the supplemental parameters for two-site model and continuously distributed site model, respectively. The basic parameters include column length, column radius, mean linear velocity of fluid, diffusion coefficient, retention factor, adsorption heat distribution parameters and so on. When pressure correction, injection correction and extracolumn correction are required, P_{in}, t_{in} and σ_{ex} need to input.

Module Deriveddata is used to calculate all parameters needed in the program from the basic parameters. Module Moment is used to calculate the moments of elution curves and used to evaluate the step size of Δp. Module Timeset is used to set the time value at which the value of elution curve is to be calculated. Certainly, the time and the step size can also be given other values, and can be adjusted according to actual results. Module Pcor is used in pressure correction, but needs much more time. Some times the working precision needs to set higher value.

In Eq. (21), k'_{aj} is choosen as a basic parameter. But we would rather want to calculate the elution curves from given k'. So we rewrite Eq. (21) as

$$A = -D_{sa}\omega^2 - p(1+B) \tag{C1}$$

where B is

$$B = \begin{cases} \dfrac{1}{\beta}\dfrac{k'k_d}{p+k_d} & \text{for single-sites} \\ \dfrac{1}{\beta}\displaystyle\sum_j \dfrac{k'_j k_{dj} P_j}{p+k_{dj}} & \text{for multiple-sites} \\ \dfrac{k'}{\beta g}\displaystyle\int \dfrac{\alpha'(Q)P(Q)}{p+k_d}dQ & \text{for continuous-sites} \end{cases} \tag{C2}$$

in which

$$g = \int \frac{\alpha'(Q)}{k_d(Q)} P(Q)dQ \tag{C3}$$

$P(Q)$ is denoted by fp[Q] in the code.

Module Elution is the main module. The whole program is: Basicdata; (Basicdata1 or Basicdata2); Deriveddata; Moment;Timeset; Pcor; Elution.

```
(*calculate elution curves*)
Elution := Module[{x}, x = 0; Print[Dynamic["completed:    "], Dynamic[100 x],
    Dynamic[" %"]]; (*find f̃_{η_s1 τ_s1}(ω,p), i.e.fs*)
   fs = π*R*v*y[r] /. DSolve[{Dsr*(y''[r] + 1/r*y'[r]) + A*y[r] == 0,
         y'[R + dl] == 0, -Dsr*y'[R] == (1 - π*R*v*y[R]) / (2*π*R)}, y[r],
       r][[1]] /. r → R // Simplify; (*find f̃_{η_m τ_m}(ω,p), i.e.fm*)
   ym[r_] = y[r] /. DSolve[{Dmr*(y''[r] + 1/r*y'[r]) + (A1 - A2*r^2)*y[r] == 0},
      y[r], r][[1]] /. C[1] → 0;
   fm = π*R*v*ym[R] /. Solve[Dmr*ym'[R] == (1 - π*R*v*ym[R]) / (2*π*R),
      C[2]][[1]] // Simplify; (*construct f̃_{ητ}(ω,p), i.e.fsm*)
   fsm = (ϵ*fs + 1 - ϵ)*fm; (*find ω(p)*)ω1 = Table[0, {20000}]; j = 1;
   While[(0 ≥ Im[ω1[[j]]] > Log[10.^-25]/L) && j < Length[ω1], ωini = Which[j < 2,
     -(Δp*(1 + kp + β))/u, j < 3, -ω1[[j - 1]] + 2*ω1[[j]], True, ω1[[j - 2]] -
     3*ω1[[j - 1]] + 3*ω1[[j]]];
    If[type == 3 && σQ > 0, B = kp/(β*g)*NIntegrate[fp[Q]*αp[Q]/(p + kd) /. p → -i*Δp*j,
      {Q, Qmin, Qmax}]]; If[Pin/Pout - 1 > 10^-4, Pcor, ω1[[j + 1]] = ω
     /. FindRoot[SetPrecision[(fsm - 1 /. {A1 → -Dma*ω^2 + 2*i*u*ω - p,
        A2 → (2*i*u*ω)/R^2, A -> -Dsa*ω^2 - p*(1 + B)} /. p → -i*Δp*j), 20],
      {ω, ωini}, WorkingPrecision → 20, MaxIterations → 1000]]; x = 0.97*
     Im[ω1[[j]]]/(Log[10.^-25]/L); j++]; If[Im[ω1[[j]]] > 0, j = j - 1];
   ω1 = Take[ω1, j]; pTab = Table[-i (jj - 1)*Δp, {jj, 1, j}]; (*find the Laplace
    transform of peak profile,f1*)f1 = e^(-i*ω1*L)*fin[pTab]*e^(σex^2*pTab^2/2);
   (*calculate peak profile, ft*)
   ft = Table[{tTab[[jj]], Δp/π*Re[f1.e^(pTab*tTab[[jj]]
      - 0.5]}, {jj, 1, Length[tTab]}]; x = 1.; (*print peak profiles*)
   ListLinePlot[ft, PlotRange → All, AxesOrigin → {0, 0}, InterpolationOrder → 2]];

(*input basic parameters*)
Basicdata := Module[{}, type = 1; L = 20 10^2 (*cm*); Dm = 0.1 (*cm^2/s*);
   u = 50.0 (*cm/s*); R = 0.01 (*cm*); ϵ = 0.6; δl = 0.2; v = 400 × 10^2 (*cm/s*);
   kp = 2; kd = 10^6 (*s^-1*); Pin = 1.0; σex = 0.2 (*s^2*); tin = 0. (*tin=t_in/t_m*);];
```

```
(*input supplemental parameters for two-site case*)
Basicdata1 := Module[{}, type = 2; kp1 = 2; kp2 = 20; kd1 = 10^8; kd2 = 0.1; P2 = 0.06];

Basicdata2 := Module[{}, type = 3; Rconst = 1.987 × 10^-3 (*gas constant,kcal/K*);
    T = 293(*K*); Q1 = 4.0(*kcal*); Q2 = 20.0(*kcal*); Qp = 7(*kcal*);
    σQ = 100.0(*kcal^2*); τ0 = 10.^-13(*s*); (*set α'(Q),i.e.αp[Q] in the code*)
    αp[Q_] := 1; (*set the distribution function of adsorption heat P(Q),
    i.e. fp[Q] in the code*)
    fp[Q_] := Piecewise[{{0, Q < Q1 || Q > Q2}, {e^-((Q-Qp)^2/(2*σQ^2)), Q1 ≤ Q ≤ Q2}}];];
(*calculate the derived parameters*)
Derivedata := Module[{j}, If[! NumericQ[tin], tin = 0]; If[! NumericQ[σex],
    σex = 0]; If[! NumericQ[Pin], Pin = 1]; Pout = 1; Dmr := Dm; Dma := Dm;
    Dsr := Dm / 3; Dsa := Dm / 3; β = δl * (δl + 2) * ε; dl = R * δl; Which[type == 1,
    B = (kp * kd)/(β * (p + kd)); k1 = β; kdw[j_] := kd^j; kd1 = 10.^20, type == 2, P1 = 1 - P2;
    kp = kp1 * P1 + kp2 * P2; B = 1/β * (kp1 * kd1 * P1/(p + kd1) + kp2 * kd2 * P2/(p + kd2)); k1 = β + kp1 * P1;
    kdw[j_] := kp / (kp1 * (1 - P2) / kd1^j + kp2 * P2 / kd2^j), type == 3, Clear[kd];
    kd := τ0^-1 * e^-(Q/(Rconst*T)); If[σQ > 0, Qmin = Max[Q1, Qp - 10 * σQ]; Qmax = Min[Q2,
      Qp + 10 * σQ]; g = NIntegrate[fp[Q] * αp[Q] / kd, {Q, Qmin, Qmax}]; kdw[j_] :=
      g / NIntegrate[fp[Q] * αp[Q] / kd^(j+1), {Q, Qmin, Qmax}], Q = Qp; g = (kp * kd)/(β * (p + kd));
      kdw[j_] := kd^j;]]; If[Pin / Pout - 1 > 10^-4, P[z_] := √(Pin^2 - (Pin^2 - Pout^2) * z / L);
    u0 = u; Dm0 = Dm; Clear[u, Dm]; u := u0 * Pout/P[z]; Dm := Dm0 * Pout/P[z]; nz = 40
    (*nz:the column is devided
      into nz section,nz must be a even number*); Δz = L / nz;
    ω2 = Table[0, {20000}, {nz + 1}]; w0 = Table[Which[jj == 1 || jj == nz + 1,
      1, EvenQ[jj], 4, OddQ[jj] && 1 < jj < nz, 2], {jj, 1, nz + 1}]];
    (*set the Laplace
    transform of inject function, f̃in(p), denoted by fin[p]*)
    fin[p_] := Piecewise[{{1, tin == 0 || p == 0}, {(1 - e^-p*tin*tm)/(p * tin * tm), tin > 0 && p ≠ 0}}];
    SetAttributes[fin, Listable];];
(*set the time values*)
Timeset := Module[{jj, j}, tTab = Select[Union[Table[t, {t, tR - 10 * σ,
      tR - 2 * σ, σ / 3}], Table[t, {t, tR - 2 * σ, tR + 2 * σ, σ / 10}],
    Table[t, {t, tR + 2 * σ, tR + 10 * σ, σ / 3}]], tm ≤ # < tR + 10 * σ &];
  If[NumericQ[n] && n < 20, tTab = Union[tTab, Table[t, {t, tR1 - 4 * σ1,
      tR1 + 4 * σ1, σ1 / 3.1}], Table[t, {t, tR1 - 2 * σ1, tR1 + 2 * σ1, σ1 / 10.1}],
    Table[t, {t, tR1 - σ1 / 4, tR1 + σ1 / 4, σ1 / 20}]]]; jj = Length[tTab]; j = 1;
  While[j < jj, If[tTab[[j + 1]] - tTab[[j]] < If[NumericQ[σ1], σ1 / 40, σ / 40],
    tTab = Delete[tTab, j + 1]; jj -= 1, j += 1];];];
```

```
(*calculate the moments*)
Moment := Module[{c2
    , c3, c21}, tm = NIntegrate[1 / u, {z, 0, L}]; Which[type == 1,
    n = tm * kp * kd, type == 2, n = tm * kp2 * P2 * kd2;]; k = kp + β; tR = (1 + k + tin / 2) tm;
  c2 := (2 * (1 + k)^2 * (Dma + β * Dsa) / u^2 + (1 + 6 k + 11 k^2) * R^2 / (24 * Dmr) + k^2 * R * dl / (3 * ϵ * Dsr) + 2 * kp / kdw[1]) / u;
  σ = (σex^2 + (tin * tm)^2 / 12 + NIntegrate[c2, {z, 0, L}])^(1/2);
  If[NumericQ[n] && n < 20, tR1 = (1 + k1 + tin / 2) * tm;
   c21 := (2 * (1 + k1)^2 * (Dma + β * Dsa) / u^2 + (1 + 6 * k1 + 11 * k1^2) * R^2 / (24 * Dmr) + k1^2 * R * dl / (3 * ϵ * Dsr) +
      2 * (k1 - β) / kd1) / u; σ1 = (σex^2 + (tin * tm)^2 / 12 + NIntegrate[c21, {z, 0,
      L}])^(1/2);];
  c3 := 1/u (12 * (1 + k)^3 * (Dma + β * Dsa)^2 / u^4 + 1/u^2 * (12 * (1 + k) * kp * (Dma + β * Dsa) / kdw[1] +
      2 * k * (1 + k) * R * dl * ((1 + 2 * k) * β * Dsa + k * Dma) / (ϵ * Dsr) + 1/(2 * Dmr) * (1 + k) * R^2 *
       ((2 + 10 * k + 11 * k^2) * β * Dsa + (1 + 5 * k + 7 * k^2) * Dma)) +
     (3 + 37 * k + 165 * k^2 + 251 * k^3) * R^4 / (960 * Dmr^2) + k^2 * (3 + 11 * k) * R^3 * dl / (24 * ϵ * Dsr * Dmr) + 2 * k^3 * dl^4 / (5 * (ϵ * Dsa)^2) +
     (3 + 11 * k) * R^2 * kp / (4 * kdw[1] * Dmr) + 2 * k * kp * R * dl / (kdw[1] * ϵ * Dsr) + 6 * kp / kdw[2]);
  M3 = NIntegrate[c3, {z, 0, L}]; skew = M3 / σ^3; Δp = 2 * π / (tR + 11 * σ);];
(*make presure correction*)
Pcor := Module[{jj}, Do[z = (jj - 1) * Δz; ωini = Which[j < 2, -Δp * (1 + kp + β) / u,
    j < 3, -ω2[[j - 1, jj]] + 2 * ω2[[j, jj]], True, ω2[[j - 2, jj]] - 3 * ω2[[j - 1,
     jj]] + 3 * ω2[[j, jj]]]; ω2[[j + 1, jj]] = ω /. FindRoot[SetPrecision[
     (fsm - 1 /. {A1 → -Dma * ω^2 + 2 * i * u * ω - p, A2 → 2 * i * u * ω / R^2, A -> -Dsa * ω^2 -
         p * (1 + B)} /. p → -i * Δp * j), 40], {ω, ωini}, WorkingPrecision → 40,
    MaxIterations → 1000] (*;Print["jj=",jj]*), {jj, 1, nz + 1}];
  ω1[[j + 1]] = w0.ω2[[j + 1]] / (3 * nz);];
```

References

[1] J.C. Giddings, H. Eyring, J. Phys. Chem. 59 (1955) 416.
[2] J.C. Giddings, J. Chem. Phys. 26 (1957) 169.
[3] A. Cavazzini, M. Remelli, F. Dondi, A. Felinger, Anal. Chem. 71 (1999) 3453.
[4] A. Felinger, A. Cavazzini, M. Remelli, F. Dondi, Anal. Chem. 71 (1999) 4472.
[5] A. Felinger, A. Cavazzini, F. Dondi, J. Chromatogr. A 1043 (2004) 149.
[6] L. Pasti, A. Cavazzini, A. Felinger, M. Martin, F. Dondi, Anal. Chem. 77 (2005) 2524.
[7] D.A. McQuarrie, J. Chem. Phys. 38 (1963) 437.
[8] F. Dondi, A. Betti, G. Blo, C. Bighi, Anal. Chem. 53 (1981) 496.
[9] F. Dondi, Anal. Chem. 54 (1982) 473.
[10] Y. Chen, J. Radioanal. Nucl. Chem. A 123 (1988) 667.
[11] Y. Chen, J. Chromatogr. A 1144 (2007) 221.
[12] Y. Chen, Y. Tan, J. Chromatogr. A 1216 (2009) 1132.
[13] J.C. Giddings, J. Chem. Ed. 35 (1958) 588.
[14] K. Yamaoka, T. Nakagawa, J. Chromatogr. 100 (1974) 1.
[15] M.J.E. Golay, Anal. Chem. 40 (1968) 382.
[16] J.H. de Boer, The Dynamical Character of Adsorption, Oxford University Press, London, 1953, pp.4–45.
[17] J.C. Giddings, J. Chromatogr. 5 (1961) 46.
[18] F. Dondi, A. Cavazzini, M. Martin, Adv. Chromatogr. 43 (2005) 179.
[19] A.T. James, A.J.P. Martin, Analist 77 (1952) 915.
[20] M.J.E. Golay, in: D.H. Desty (Ed.), Gas Chromatography, Butterwort, London, 1958, pp. 36–53.
[21] G.H. Stewart, S.L. Seager, J.C. Giddings, Anal. Chem. 31 (1959) 1738.
[22] J.C. Giddings, Anal. Chem. 36 (1964) 741.
[23] J.C. Sternberg, in: J.C. Giddings, R.A. Keller (Eds.), Advances in Chromatography, 2, Marcel Dekker, New York, 1966, pp. 205–270.
[24] S.P. Cram, T.H. Glenn Jr., J. Chromatogr. 112 (1975) 329.